Demonstration of Auxiliary Management and Control Channel Signal Transmission for FDM Coherent Passive Optical Network

Jiaye Wang
Key Laboratory of EMW Information (of Fudan University)
Shanghai, China
21210720227@m.fudan.edu.cn

Wangwei Shen
Key Laboratory of EMW Information (of Fudan University)
Shanghai, China
wwshen21@m.fudan.edu.cn

Jiang Chen
Key Laboratory of EMW Information (of Fudan University)
Shanghai, China
20210720083@fudan.edu.cn

Guoqiang Li
Key Laboratory of EMW Information (of Fudan University)
Shanghai, China
19210720066@fudan.edu.cn

Sizhe Xing
Key Laboratory of EMW Information (of Fudan University)
Shanghai, China
szxing21@m.fudan.edu.cn

Jianyang Shi
Key Laboratory of EMW Information (of Fudan University)
Shanghai, China
jy_shi@fudan.edu.cn

Nan Chi
Key Laboratory of EMW Information (of Fudan University)
Shanghai, China
nanchi@fudan.edu.cn

Junwen Zhang
Key Laboratory of EMW Information (of Fudan University)
Shanghai, China
junwenzhang@fudan.edu.cn

***Abstract*—For the first time, we proposed and demonstrated auxiliary management and control channel (AMCC) in frequency division multiplexing coherent passive optical network (FDM-PON) based on digital subcarriers (DCM) to transmit control information and reduce the latency of signal transmission. We propose an extraction algorithm to detect AMCC signals. A 4-band FDM QPSK coherent PON system of a total 100-Gbps data rate with a 24-Mbps non-return-to-zero (NRZ) signal was demonstrated and the system performance at different modulation index (MI) was analyzed.**

Keywords*—*Coherent PON, FDM, AMCC.

I. Introduction

In recent years, with the rapid development of fifth-generation (5G) mobile communication network, cloud services, virtual reality (VR) applications and edge computing, user data traffic is increasing at a tremendous rate, so higher requirements are required on passive optical network (PON), such as higher data transmission rates, wider coverage and lower latency [1]. Traditional PONs are based on intensity modulation and direct detection (IM/DD) in the physical layer, but the sensitivity, power prediction, and limited transmission rate of O-band IM/DD PON cannot meet the needs. Therefore, the C-band coherent PON can be most favorable candidate for the challenges [2]. Compared with the IM/DD system, the coherent PON provides faster data rate, gains adequate power budget with a modest transmitting power and enables the efficient utilization of digital signal processing (DSP) algorithms [3]. Additionally, more flexibilities are enabled by coherent PON, i.e., frequency division multiplexing (FDM), for multi-user access [4].

High-speed coherent PONs demand stringent latency in 5G. In the traditional time-division multiplexing passive optical network (TDM-PON), conventional dynamic bandwidth allocation schemes and the quiet window for ONU registration increase the overall latency which is beyond the allowable delay range of 5G [5]. Owing to the quiet window, the discovery and registration processing between ONU and OLT cause high latency to TMD-PON [6]. Due to the common public radio interface (CPRI) [7] in a wavelength division multiplexing passive stringent network (WDM-PON), the quiet window is unfeasible. In order to transmit control information with low latency in the WDM-PON, auxiliary

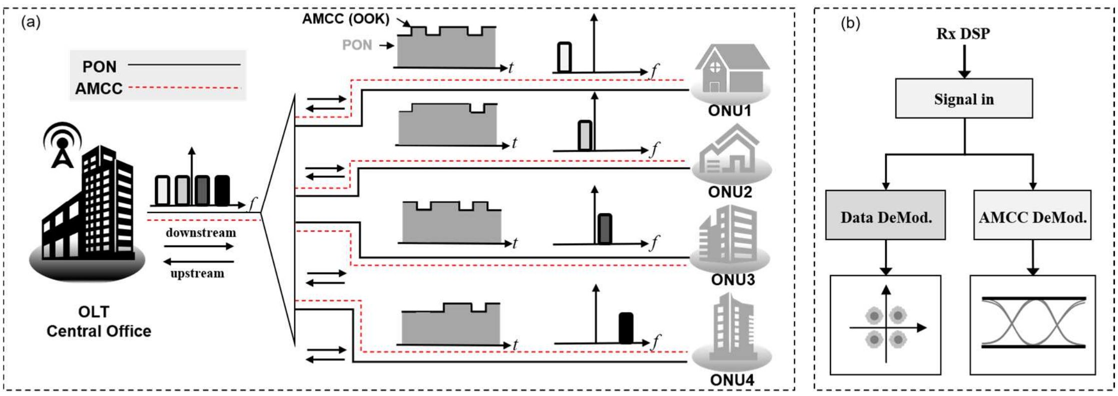

Fig. 1. (a) Architecture diagram of FDM-PON with AMCC. (b) The Rx DSP of the main data and AMCC.

XXX-X-XXXX-XXXX-X/XX/$XX.00 ©20XX IEEE

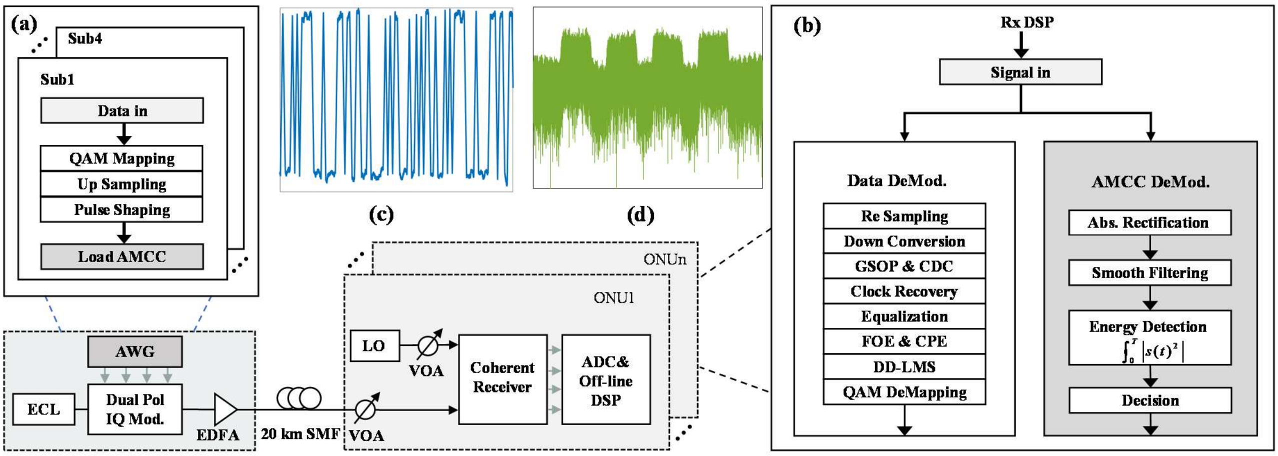

Fig. 2. Experimental setup for coherent FDM PON with AMCC. (a) and (b) are the Tx and Rx DSP; (c) The waveform diagram in the time domain; (d) The spectrum of 4-band FDM-PON signal.

management and control channel (AMCC) is proposed [8,9]. In [8], Guo et al. directly control the DC bias of the MZM to achieve AMCC transmission. In [9], Ryo et al. utilize a 3-step moving averaging method based DSP block to extract AMCC signals from the main signals. Referring to the control information transmission in WDM-PON, we believe that AMCC can also be an effective method for low latency operations in a coherent FDM-PONs. However, as far as we know, no experiments have demonstrated the feasibility of AMCC in a FDM-CPON.

In this paper, we proposed AMCC for coherent FDM-PON to transmit control information with low latency for the first time. Moreover, we demonstrated an effective extraction algorithm to detect AMCC signals. To extract the AMCC signal from the main signal, we utilized smooth filtering and energy detection for the decision of non-return-to-zero (NRZ) symbols. We demonstrated a 4-band FDM QPSK coherent PON system of a total 100-Gbps data rate with a 24-Mbps NRZ-AMCC signal. Additionally, we analyzed the system performance at different modulation indexes (MI) in this experimental demonstration.

II. Principles and Experimental Setup

Fig. 1 shows the principle of the coherent FDM-PON with AMCC. Coherent FDM-PON allocates a digital subcarrier (DCM) exclusively to each user on one wavelength so that it can save the wavelength resources and achieve the requirement of a large-capacity network. At the transmitter end, the main information for each user is modulated into the corresponding sub-carrier. Then the main sub-carrier signal is re-modulated with the AMCC signal on the envelope of the main sub-carrier signal. In other words, the AMCC is a kind of amplitude modulation to the main signal. Compared with the main signal of a high data rate, the AMCC signal is a narrow-band NRZ signal of a quite low data rate. Note that the AMCC signal is generated for each user (sub-band) separately. The AMCC signal can be transmitted both in the up-link and the down-link. At the receiver end, we process the received signal in two separate branches, i.e. the AMCC signal DSP and the main data DSP. At the branch of AMCC signal DSP, we first take the absolute value of the receiver signal to get the rectification signal. After absolute-value rectification, the signal is filtered by a smooth filter, which is a lowpass filter. After smooth filtering, we calculate the energy of each NRZ symbol period. At last, the discrete points after energy detection are decided as NRZ symbols.

Figure. 2 shows the experimental setup for coherent FDM-PON with AMCC. At the OLT side, the external cavity lasers (ECL) with the wavelength of 1553.6nm are used as signal light source, and we use four subcarriers multiplexing scheme, which subcarrier carries 6.25-GBaud PDM-QPSK signal and 24-MBaud NRZ re-modulated to QPSK signals on the envelope or amplitude. Then the four subcarriers are modulated by a dual polarization (DP) I/Q modulator and boosted by an EDFA with a launch power of 6 dBm before launched to 20km single mode fiber (SMF). At the receiver side, a variable optical attenuator (VOA) is used for adjusting the received signal power. Then the signal and LO after power adjustment by VOA are detected by an integrated coherent receiver (ICR). After that, the detected signals are captured by an 256-GSa/s digital storage oscilloscope (DSO) for offline DSP. Fig. 2(a) and (b) are the generation steps of transmission signals and the demodulation steps of receiver signals, separately. For signal generation steps, the data is first mapped to QPSK per subcarrier. Then each subcarrier signal is up-sampled for 16 times and Nyquist pulse-shaped with a roll-off of 0.1. Before sending to AWG, the NRZ signal which transmits as AMCC re-modulated to this shaped QPSK signal on the amplitude. Fig. 2(c) and (d) are time domain and spectrum diagrams of mixed signals with QPSK signal and NRZ signal, respectively. At the receiver side, each subcarrier is processed independently. The detailed operation of the QPSK signal demodulation is shown in the left side of (b). At the branch of AMCC NRZ signal demodulation, for the first step, we take the absolute value of the receiver signal to make it non-negative. After absolute-value rectification, the rectified signal is smoothed. Then the signal is detected to discrete points according to the energy of each NRZ symbol period.

III. Results

To verify the feasibility of the proposed scheme added AMCC in coherent FDM PON, we initially test the performance of PDM-QPSK signal in different modulation index (MI). Fig. 3(a) shows the calculated BER versus received optical power (ROP) with different MI under back-to-back (BTB), in all tests we notice -37.4 dBm and -34.4 dBm ROP for QPSK without AMCC at the threshold of 0.01 and 0.001. Moreover, for QPSK with 10.53% MI, we can see that

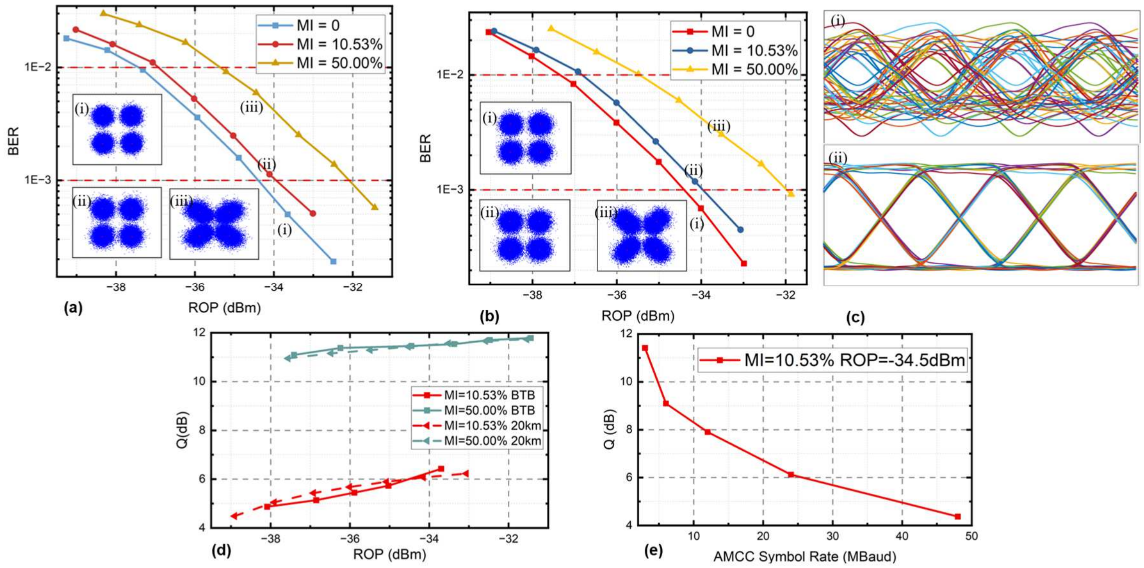

Fig. 3. The results of (a) BER versus ROP in the BTB case; (b) BER versus ROP in the 20-km case; (c) the eye diagrams of NRZ signals at the BER threshold of 0.01 when (i) MI=10.53%, (ii) MI=50%; (d) the results of Q versus ROP; (e) the results of Q versus bandwidth when MI=0.9 and ROP=-34.5dB.

the ROP is -36.9 dBm and -34 dBm at the threshold of 0.01 and 0.001.Therefore, there are 0.4 to 0.5 dB sensitivity penalty for 10.53% MI at the BER thresholds of 0.01 and 0.001. However, when the MI is 50.00%, the ROP for QPSK is -35.4 dBm and -32.1 dBm at the threshold of 0.01 and 0.001. For this case, we found there is about 2 to 2.3dBm sensitivity penalty for 50% MI at the threshold of 0.01 and 0.001, respectively. Fig. 3(b) shows the BER versus ROP with different modulation index (MI) after 20-km SMF transmission. There is slight sensitivity difference of about 0.1dB under BTB and 20km SMF. In Fig. 3(a) and (b), (i), (ii), (iii) are constellation chart with 0, 10.53% and 50.00% MI under BTB and 20km SMF, respectively. From the these constellations insets, we can find the performance of QPSK is worse as MI value becomes larger.

For AMCC, the signal eye diagrams under 10.53% and 50.00% MI values for QPSK signals at the BER threshold of 0.01 are shown in insets (i) and (ii) of Fig. 3(c). In an eye diagram, the height of the eye opening indicates the value of Q. It is clear that the performance under 50.00% MI is better than that under 10.53% MI. Q is the quality factor of the AMCC signal, and a larger Q value indicates better NRZ signal performance. The calculated Q versus ROP with different MI values under BTB transmission and 20km SMF transmission is shown in Fig. 3(f). The performance improves significantly as the value of ROP increases. There is a slight difference in Q between BTB and 20km SMF. The NRZ signal under BTB and 20km SMF both perform best with 50% MI, and the value of Q is nearly 11.3dB when the ROP is -36dBm. However, when the value of MI is 10.53%, the NRZ signal under BTB and 20km SMF both perform worse, and the value of Q is nearly 5.5dB when the ROP is -36dBm. Fig. 3(e) shows the calculated Q versus symbol rate with 10.53% MI and -34.5dBm ROP. In this figure, the value of Q decreases as the AMCC symbol rate increases.

IV. Conclusion

In this paper, we proposed and demonstrated AMCC for coherent FDM-PON to transmit control information. AMCC transmits control information by envelope modulation, which avoids additional slots and extra bandwidth, has great potential for low latency operations. We utilize smooth filtering and energy detection for the decision of NRZ symbols to extract the AMCC signal from the main signal. Finally, a 4-band FDM QPSK coherent PON system of a total 100-Gbps data rate with a 24-Mbps NRZ-AMCC signal is demonstrated.

Acknowledgment

This work is partially supported by National Natural Science Foundation of China (62171137, 62235005 and 61925104), Natural Science Foundation of Shanghai (21ZR1408700), and the Major Key Project PCL.

References

[1] J. Zhang, et al. "Rate-Flexible Single-Wavelength TFDM 100G Coherent PON based on Digital Subcarrier Multiplexing Technology," in Optical Fiber Communication Conference (OFC) 2020, paper W1E.5.

[2] J. Zhang, et al. "Efficient preamble design and digital signal processing in upstream burst-mode detection of 100G TDM coherent-PON," J. Opt. Commun. Netw. 13, A135-A143 (2021).

[3] N. Kaneda N, et al. "Coherent PON: System Merit and Technical Challenges," Opto-Electronics and Communications Conference (OECC). IEEE, 2021: 1-3.

[4] J. Zhang and Z. Jia, "Coherent Passive Optical Networks for 100G/λ-and-Beyond Fiber Access: Recent Progress and Outlook," in IEEE Network, vol. 36, no. 2, pp. 116-123 (2022).

[5] J. S. Wey and J. Zhang, "Passive Optical Networks for 5G Transport: Technology and Standards," J. Lightwave Technol. 37, 2830-2837 (2019)

[6] H. H. Lee, et al. "Demonstration of high-power budget TDM-PON system with 50 Gb/s PAM4 and saturated SOA." Journal of Lightwave Technology 39, 2762-2768 (2021).

[7] Recommendation ITU-T G.989, "40-Gigabit-capable passive optical networks (NG-PON2): Definitions, abbreviations and acronyms", 2015.

[8] H. Guo, et al. "AMCC nonlinear baseband superimposition and extraction aided by proposed interference cancellation for WDM-PON used in 5G mobile fronthaul." Optics Express, vol. 30, pp. 31602-31613 (2022).

[9] R. Igarashi, et al. "Simultaneous reception of AMCC signals and QPSK signals by a single coherent receiver with DSP." Optics Express, vol. 30, pp. 48030-48041 (2022)